Glycobiology, 2021, vol. 31, no. 7, 762–771
https://doi.org/10.1093/glycob/cwab010
Advance Access Publication Date: 5 February 2021
Original Article

Analytical Glycobiology

Glycosylation of recombinant rabbit immunoglobulins influences protease susceptibility as shown by comprehensive mass spectrometric glycan analysis

Irene Friligou[1], Jana Gassner[2], Dominic Knoblauch[1], Gabriele Kagerer[1], Franziska Popp[1], Susanne Voit[1], Alfred M Engel[1], Andreas Leinenbach[1], Wojtek Steffen[1], Markus Haberger[2] and Glòria Tabarés*[1]

[1]Department of Early Development and Reagent Design, Roche Diagnostics GmbH, Nonnenwaldstr. 2, 82377 Penzberg, Germany, and [2]Pharma Technical Development, Roche Diagnostics GmbH, Nonnenwaldstr. 2, 82377 Penzberg, Germany

*To whom correspondence should be addressed: Tel: +4988566019497; e-mail: gloria.tabares@roche.com

Received 22 August 2020; Revised 18 January 2021; Accepted 29 January 2021

Abstract

Recombinant immunoglobulins (rIgGs) have become increasingly important as therapeutic agents and diagnostic tools in recent years. Genetic engineering allows the introduction of non-natural features such as the Sortase motif for site-directed labeling. In this study, the enzyme Sortase A (SrtA) was used for the proteolytic cleavage of rIgGs to produce their biotinylated Fab fragments by locating the cleavage site close to the hinge region. However, SrtA cleavage of engineered rabbit IgGs (rRb-IgGs) derived from human embryonic kidney (HEK) 293 cells showed significantly lower yields compared with their mouse counterparts. Nonrecombinant Rb-IgGs have N- and O-glycans, and the presence of O-glycans close to the hinge region of the rRb-IgGs might affect the susceptibility of these antibodies to SrtA cleavage. In addition, the glycosylation pattern of rIgGs differs depending on the host cell used for expression. Therefore, we analyzed the N- and O-glycans of various rRb-IgGs expressed in HEK293 cells, detecting and quantifying 13 different N-glycan and 3 different O-glycan structures. The distribution of the different detected glycoforms in our rRb-IgG N-glycan analysis is in agreement with previous studies on recombinant human IgG N-glycans, confirming the hypothesis that the host cell defines the glycosylation of the recombinant produced IgGs. O-glycosylation could be mapped onto the threonine residue within the hinge region sequence XPTCPPPX, as already described previously for nonrecombinant Rb-IgGs. Substitution of this threonine allowed an almost complete Fab fragment cleavage. Therefore, we could confirm the hypothesis that the O-glycans affect the SrtA activity, probably due to steric hindrance.

Key words: immunoglobulin G (IgG), mass spectrometry, N-, O-Glycosylation, rabbit antibodies, Sortase enzymatic modification of IgG

Introduction

Antibodies such as immunoglobulin G (IgG) consist of two antigen-binding fragments (Fabs) that are linked via a flexible region (the hinge) to a constant (Fc) region which serves to bind various effector molecules of the immune system, as well as molecules that determine the biodistribution of the antibody. In addition, IgGs are sialoglycoproteins containing N- and O-complex sialylated glycans that are also crucial for their biological activity, in particular a conserved N-glycosylation site in the CH2 domain of each heavy chain of the Fc region (Sutton and Phillips 1983; Raju et al. 2000). The Fc-attached oligosaccharides are highly heterogeneous, affecting the IgG effector functionality in ways such as binding to Fc receptors and subsequent activating, or inhibiting biological and pharmacological actions (Dashivets et al. 2015, Yamaguchi and Barb 2020). For example, binding to the neonatal Fc receptor is modulated by the Fc-glycosylation pattern and correlates directly with the circulatory half-life of therapeutic antibodies in the bloodstream (Hossler et al. 2009).

Glycosylation of the antigen-binding Fab fragment was found in approximately 15–25% of human serum IgG; this may influence antigen binding. Its role in autoimmune disease and chronic inflammation is under investigation: For instance, Lloyd et al. 2018 discussed the impact of high levels of Fab glycosylation of anticitrullinated protein autoantibodies in rheumatoid arthritis patients.

Recombinant immunoglobulins G (rIgG), produced by recombinant DNA technology and/or transgenic technology, are major therapeutic agents in the treatment of cancer and other life-threatening diseases, and are also used for diagnostic purposes. Since glycosylation is cell-type specific, rIgGs produced in different host cells contain different patterns of oligosaccharides, which could affect their biological functions (Hossler et al. 2009). Another major concern of bioprocesses based on transient gene expression is the batch-to-batch variability in protein yield and quality, especially with regard to protein glycosylation (Nallet et al. 2012). Previous studies focused mainly on N-glycan analysis, and O-glycan analysis was not fully addressed.

Although our knowledge of human antibody glycosylation has been growing considerably, the immunoglobulin glycomes of important model systems have also been increasingly mapped. These include the IgG glycosylation pattern of cell lines, such as CHO, HEK, NS0 and SP2 cells, and various murine strains (de Haan et al. 2020). However, detailed analysis of the glycosylation of rabbit IgGs (Rb-IgGs) is still missing. Native, nonrecombinant Rb-IgGs feature N- and O-glycans. About 25% of the total IgGs bind to jacalin lectin, a specific lectin for O-glycosylation, indicating that only some Rb-IgG molecules are O-glycosylated, while all Rb-IgG present N-glycans.

The O-glycan structures were characterized by NMR spectroscopy, showing low heterogeneity including sialylated di- and tri-saccharides (Kabir and Gerwig 1997). The presence of those O-glycan moieties in the hinge region of Rb-IgGs might confer resistance to proteolysis, and accordingly, Rb-IgG molecules containing these O-glycans were found to be more resistant to the action of papain (Fanger and Smyth 1972b, Tsay et al. 1980).

Enzymatically cleaving proteins while introducing small chemical tags in a site-directed manner using the peptidase Sortase A (SrtA) is known as Sortagging (Popp et al. 2007). The method has found broad use in protein engineering, for preparing bioconjugates for diagnostic purposes, as well as in the generation of therapeutic antibody-drug conjugates (Beerli and Grawunder 2017). Introduced above or below the IgG hinge region, Sortagging allows the generation of labeled Fab or F(ab')2 fragments, respectively.

The present study describes the structure and binding site of N- and O-glycans of recombinant rabbit IgGs (rRb-IgGs) expressed in HEK293 cells using different complementary enzymatic and mass spectrometric methods. In addition, we discuss the observation of their resistance to Sortagging in cases where the cleavage site is in close proximity to the O-glycan attachment site.

Results

Characterization of rRb-IgG O-glycans and site mapping

O-Glycans were released from two different rRb-IgG F(ab′)2 fragments by β-elimination, subsequently permethylated and analyzed by nanospray ionization mass spectrometry (MS). A monoclonal mouse F(ab′)2 was used as negative control, since mouse monoclonal IgG1 antibodies do not feature O-glycans (Köhler et al. 1978). The removal of the Fc-part of all analyzed IgGs, where the N-glycans are bound, confirmed that the observed glycans are O-glycans only. The generated full MS of the two different rRb-IgG F(ab′)2 fragments allowed for the detection of those released O-glycans: GalNAc(1)Gal(1)Neu5Ac(1) and GalNAc(1)Gal(1)Neu5Ac(2). Identification of the O-glycans was based on comparing the theoretical mass with the experimental mass. Furthermore, an MS/MS experiment for confirming GalNAc(1)Gal(1)Neu5Ac(1) was performed, which showed characteristic MS/MS signals for the respective glycans (data not shown). As expected, no O-glycans were found in the negative control.

Based on these findings, four different rRb-IgGs, produced by the same expression system but of different antibody specificities, were digested with trypsin and analyzed by RP-UPLC-ESI MS for the identification of the O-glycosylation site and relative quantification of the different O-glycan species at the glycopeptide level. The O-glycans were found to be attached onto Thr_{104} (numbering according to UniProtKB P01870, IGHG_RABIT) within the hinge region sequence XPTCPPPX. The most abundant linked O-glycan was found to be the disialylated core 1 structure GalNAc(1)Gal(1)Neu5Ac(2) (m/z 1065.2629, z = 4; Figure 1; Table I). We were also able to find masses that correspond to the monosialylated core 1 structure GalNAc(1)Gal(1)Neu5Ac(1) (m/z 992.4883, z = 4; Figure 1) and to the desialylated core 1 structure GalNAc(1)Gal(1) (m/z 919.7141, z = 4; Figure 1). No masses corresponding to the O-glycans with Neu5Gc (NGNA) sialic acids could be detected. Table I includes a list of all three O-glycan structures observed together with their relative abundances in the four different rRb-IgG clones analyzed. The peptide with the amino acid motif XPTCPPPX was found to be glycosylated at approximately 40–50% in all four rRb-IgGs and the disialylated core 1 structure GalNAc(1)Gal(1)Neu5Ac(2) was found to represent approximately 90% of the total found O-glycan structures.

The O-glycan attachment position was additionally determined via intact HPLC-ESI MS analysis of cleavage products after digestion of the rRb-IgGs by OpeRATOR™, an O-glycan-specific protease. MS data showed that rRb-IgG digestion occurred N-terminally of Thr_{104} within the amino acid motif XPTCPPPX, confirming our previous results.

O-Glycans were detected in one or both heavy chains of rRb-IgG at the described position; however, some rRb-IgGs presented no

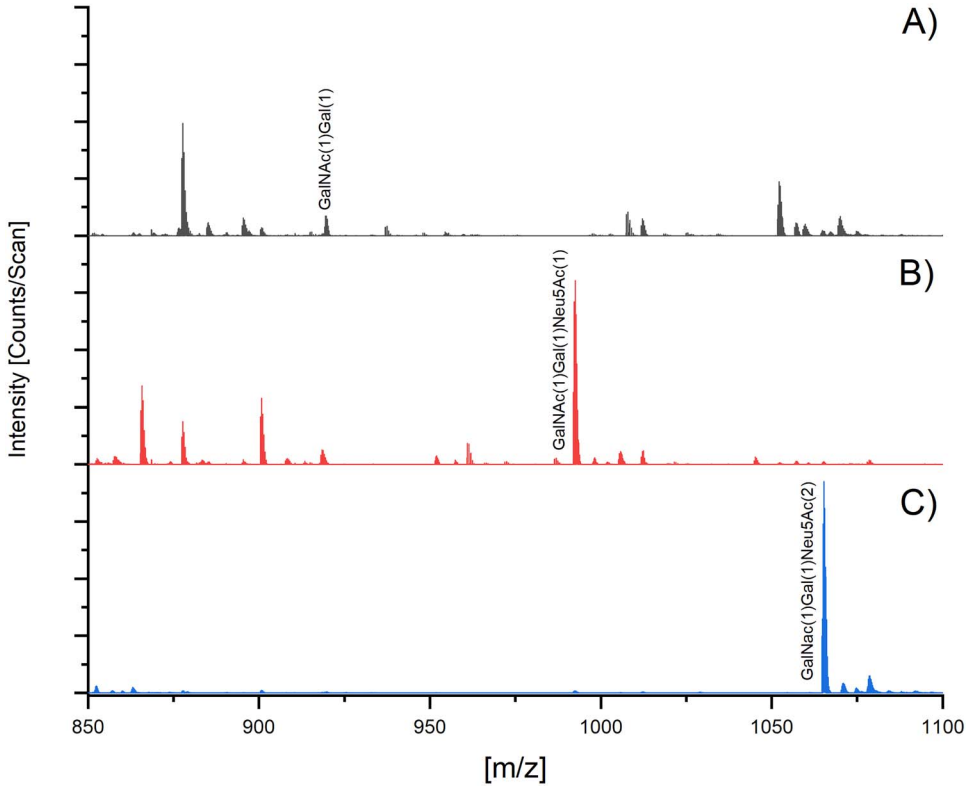

Fig. 1. Mass spectra of tryptic O-glycopeptide signals, at charge state 4. (A) without sialic acids (for visualization signals are enlarged, *y* values multiplied by 10) eluting at retention time 31.35–31.83 min, (B) O-glycopetide with one sialic acid, eluting at retention time 32.66–33.37 min and (C) O-glycopepitde with two sialic acids eluting at retention time 33.74–34–78 min in tryptic LC–MS analysis. Monosaccharide symbols follow the SNFG (symbol nomenclature for Glycans) system (PMID 26543186, *Glycobiology* 25:1323–1324, 2015) details at NCBI.

O-glycans on their heavy chains. No activity of the OpeRATOR™ protease was detectable by LC–MS when applied on mouse IgG, used as negative control.

Characterization of rRb-IgG N-glycans and site mapping

In addition, we checked the peptide maps of the above four rRb-IgGs for their N-glycosylation profiling: the N-glycans were located on the Fc-part of the heavy chain, attached to the Asn_{173} of the peptide EQQFNSTIR within the CH2-domain. Identification of glycopeptides was again based on MS1 signals comparing theoretical mass to experimental mass (for details, refer Materials and methods). The peptide was mainly present in its glycosylated form (>98% of total peptide). The most abundant linked N-glycan comprising approximately 57–67% of the total found N-glycan structures is the complex-type biantennary core-fucosylated G0F glycan (m/z 1284.5498, $z = 2$; Figure 2; Table II), followed by the G1F, comprising approximately 21–28% (m/z 1365.5761, $z = 2$; Figure 2; Table II). Furthermore, high-mannose type, as well as monoantennary and bisecting N-glycans were present, but in smaller amounts. Some of the low abundant biantennary N-glycans featured one terminal Neu5Ac (NANA) sialic acid, whereas no terminal Neu5Gc (NGNA) sialic acids were detected.

SrtA mediated labeling

For site-specific conjugation, a Sortase motif LPETG was inserted between Ser_{101} and Lys_{102} directly upstream of the K_{102}PTCPPP motif. Subsequent SrtA incubation yielded only little Fab-biotin product (Figure 3); approximately 5% of the starting material resulted as purified biotinylated Fab fragment. After desialylation of the IgG, SrtA reaction yields increased by a factor of approximately 5 (Figure 3), with 23% weight yield of the purified fragment. The relative intensities of O-glycan patterns containing one or two remaining sialic acids were considerably higher in the unreacted heavy chain than in the processed Fc-part after the SrtA reaction (Figure 4).

When performing the SrtA reaction on the mutant MAb <xxx>rRb-4H11(T_{104}A)-IgG, with the hinge Thr_{104} adjacent to the SrtA tag insertion being substituted by Ala, almost complete processing to the Fab-biotin product could be achieved. The calculated weight yield of purified biotinylated Fab fragment was 52% compared with the starting amount of IgG, i.e. a ~10-fold increase compared with the original construct (Figure 3).

As a control, the desialylation reaction was performed on a rabbit/mouse chimera, MAb<xxx>rRb/M-4H11-IgG, containing an SrtA tag in the lower hinge region, but comprising a mouse IgG backbone without any O-glycosylation sites. The routinely very high yields of Fab-SrtA conjugates in the control rRb/M-IgG were not affected by the desialylation conditions (data not shown).

Discussion

The N-glycan structures of natural, nonrecombinant Rb-IgG and HEK293-derived rRb-IgG are different, as shown during the course of the study. Nonrecombinant Rb-IgGs have been described as

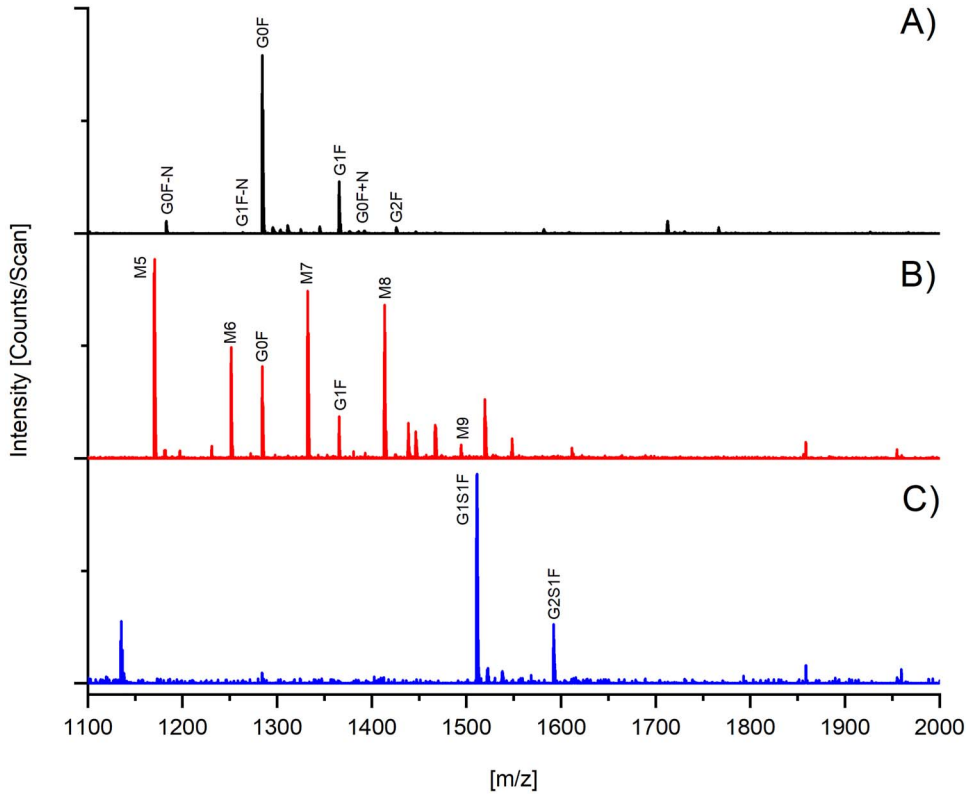

Fig. 2. Mass spectra of tryptic N-glycopeptide signals, at charge state 2. (A) main species G0F, G1F and G2F eluting at retention time 11.13–11.46 min, (B) high-mannose species M5, M6, M7 and M8 (for visualization signals are enlarged, *y* values multiplied by 5), eluting at retention time 10.50–10.97 min and (C) sialic acid containing species G1S1F and G2S1F (for visualization signals are enlarged, *y* values multiplied by 10) eluting at retention time 11.92–12.26 min in tryptic LC–MS analysis. Monosaccharide symbols follow the SNFG (symbol nomenclature for Glycans) system (PMID 26543186, *Glycobiology* 25:1323–1324, 2015) details at NCBI.

possessing oligosaccharides located at three different sites on the heavy chain (Fanger and Smyth 1972b): the main N-glycosylation site within the CH2-domain of IgG via an asparagine residue is present in all Rb-IgG heavy chains, whereas a second O-glycan structure via a threonine (close to the hinge region) is present in 40% of the heavy chains analyzed and a third, less abundant structure, via an asparagine on the Fd-part of the heavy chain, close to the disulfide bridge, linking light and heavy chains.

Raju et al. (2000) described the N-linked carbohydrates detected in all nonrecombinant IgG molecules from 13 different species and showed a heterogeneous array of biantennary complex-type oligosaccharides. Moreover, a species-specific variation in core fucosylation and terminal galactosylation was reported. They could not detect any hybrid or complex tri- and tetra-antennary structure. Particularly for Rb-IgG structures, the N-glycans were mostly of the complex-type without core fucose, whereas no high-mannose type was detected.

Taniguchi et al. (1985) described asparagine-linked glycans distributed in both the Fc and Fab fragments of Rb-IgG. The glycans consisted of 16 different biantennary complex-type sugar chains that have one of the four different core structures of (±GlcNAc)(±Man)Man(2)GlcNAc(1)(±Fuc)GlcNAc(1). These cores were also present in different amounts in human IgGs (Mizuochi et al. 1982). The glycans of the Fab fragments were found to be desialylated, monosialylated and disialylated, whereas the glycans of the Fc fragments were only desialylated and monosialylated. In addition, the Fab fragment glycans contained more galactose and bisecting N-acetyloglucosamine than the glycans from Fc fragments.

After exhaustive glycan analysis of rRb-IgGs expressed in HEK293 cells, we found one N- and one O-glycosylation site in each heavy chain but no second N-glycosylation site could be identified, in contrast to Fanger and Smyth (1972b) as well as Taniguchi et al. (1985). The N-glycans were mainly biantennary complex-type, however, in contrast to natural Rb-IgGs (Raju et al. 2000) which are mostly (>57%) core fucosylated (G0F). Furthermore, we could not detect any tri- or tetra-antennary nor any hybrid N-glycan structures, confirming the observations of Patel et al. (1992) and Raju et al. (2000). However, in contrast, we were able to detect low abundant high-mannose type N-glycans on the IgGs. Moreover, the biantennary core-fucosylated N-glycans were found to be mainly desialylated, leaving only a small percentage monosialylated (Table II). Bisecting N-glycans were detected, as previously described for nonrecombinant Rb-IgGs by Raju et al. (2000). We found only NANA sialic acid, and no NGNA.

Nallet et al. (2012) detected 11 different N-glycans in an HEK293-derived human IgG, but only four contributed to >98% of the forms, those being G1F (58.5%), G2F (20.8%), G0F (14.3%) and the mixed complex forms (4.1%) including high-mannose and monoantennary structures. In our analysis of HEK293-expressed rRb-IgGs we found 13 different N-glycan structures with the main four forms being G0F (~60%), G1F (~25%), G2F (~4%) and G0F-N (~4%). The rest of the identified N-glycans were

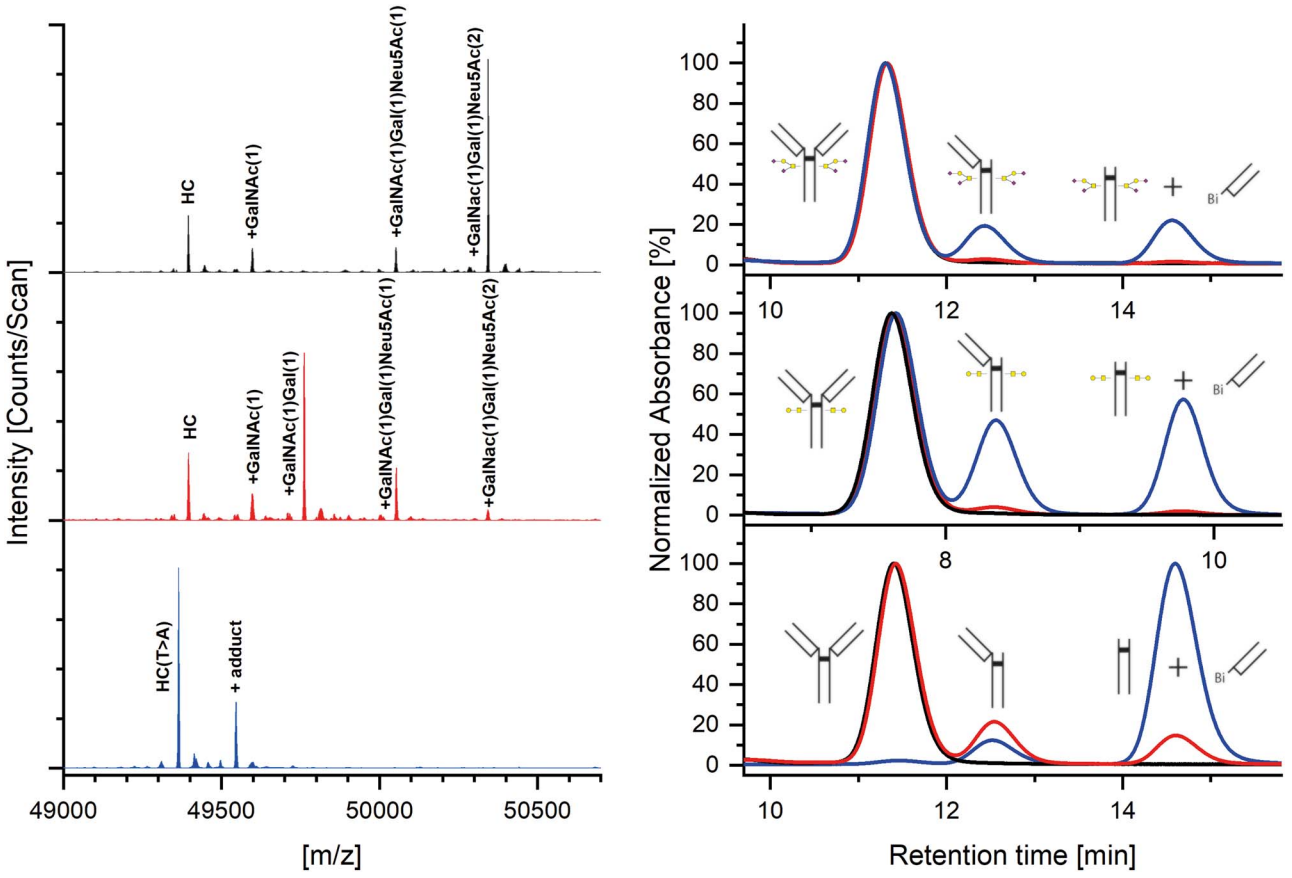

Fig. 3. Mass spectra and HPLC profiles after SrtA reaction. Presence of hinge O-glycans lead to low performance of the SrtA reaction. Left panel: HPLC–MS analysis of N-deglycosylated and reduced (top), desialylated, N-deglycosylated and reduced (middle) MAb<xxx>rRb-4H11-IgG (SrtA upper hinge), and of deglycosylated and reduced MAb<xxx>rRb-4H11(T > A)-IgG (SrtA upper hinge) containing a single amino acid substitution (bottom). Deconvoluted heavy chain (HC) spectra are shown. Right panel: size exclusion chromatograms of MAb<xxx>rRb-4H11-IgG (top), desialylated MAb<xxx>rRb-4H11-IgG (middle) and MAb<xxx>rRb-4H11(T > A)-IgG containing a single amino acid substitution (bottom) illustrating the product formation of the SrtA reaction at *t* = 0 h (black), 1 h (red) and 18 h (blue). *Y*-axes of chromatograms are normalized from 0 to 100. Main glycosylation forms are illustrated, monosaccharide symbols follow the SNFG (symbol nomenclature for Glycans) system (PMID 26543186, *Glycobiology* 25:1323–1324, 2015) details at NCBI.

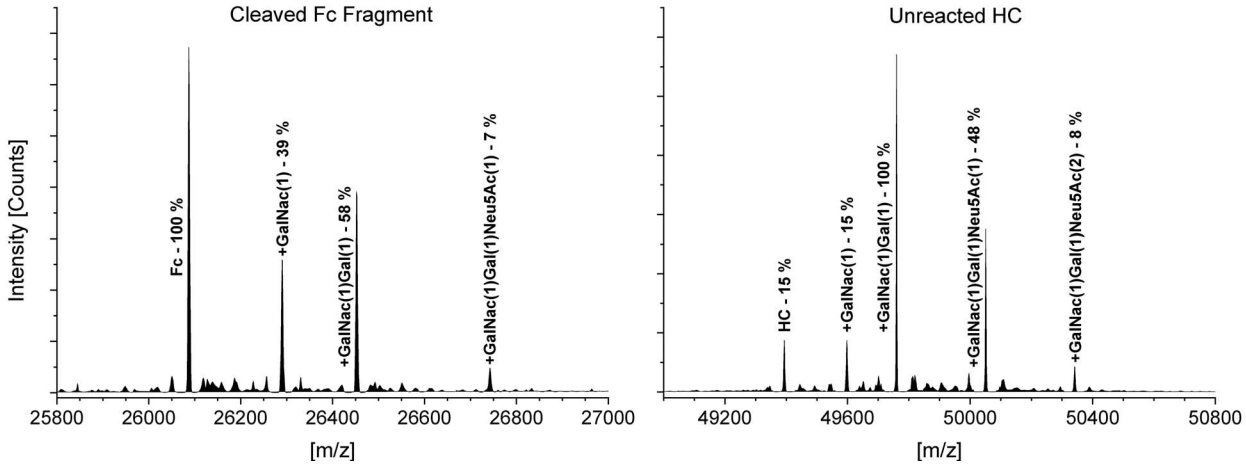

Fig. 4. Mass spectra of O-glycan distribution in SrtA cleaved versus noncleaved reaction products of desialylated IgG. HPLC–MS analysis of SrtA reaction products (left panel; Fc-part) and unreacted antibody (right panel) of desialylated, N-deglycosylated and reduced MAb<xxx>rRb-4H11-IgG (SrtA upper hinge) after SrtA reaction. Deconvoluted HC spectrum is shown, relative intensities of O-glycans in percentage compared to main form are indicated. Main glycosylation forms are illustrated, monosaccharide symbols follow the SNFG (symbol nomenclature for Glycans) system (PMID 26543186, *Glycobiology* 25:1323–1324, 2015) details at NCBI.

Table I. O-glycosylation site and glycan structures after HPLC–MS analysis of the tryptic digested O-glycan containing peptides including relative amounts. Monosaccharide symbols follow the SNFG (symbol nomenclature for Glycans) system (PMID 26543186, *Glycobiology* 25:1323–1324, 2015) details at NCBI

O-linked glycan structure	O-linked glycan nomenclature	Theoretical monoisotopic mass of the (glyco-) peptides (Da)	Relative abundance [%]			
			MAb<xxx>rRb-1G9-IgG	MAb<xxx>rRb-1A4-IgG	MAb<xxx>rRb-3G3-IgG	MAb<xxx>rRb-2F2-IgG
Peptide XPTCPPPX (nonglycosylated)	-	3307.69	47.1	51.0	43.3	50.0
Peptide	GalNAc(1)Gal(1)	3672.82	0.4	0.6	0.4	0.7
Peptide	GalNAc(1)Gal(1)Neu5Ac(1)	3963.91	3.7	3.5	4.0	3.6
Peptide	GalNAc(1)Gal(1)Neu5Ac(2)	4255.01	48.8	44.9	52.4	45.8

five different monoantennary, biantennary and bisecting complex N-glycans (~0.1–1%) and four different forms of high-mannose type N-glycans (~0.1–1%). The distribution of the different detected glycoforms in our rRb-IgG N-glycan analysis is very close to the results of the recombinant human IgG N-glycan analysis described by Nallet et al. (2012): both IgGs from different species but produced in HEK293 cells confirming the hypothesis that the host cell defines the glycosylation of the recombinant produced IgGs. Moreover, the sialic acid types detected on the N-glycan structures of endogenous human IgG do not contain any NGNA sialic acid type, only NANA, whereas NGNA dominates in the case of nonrecombinant Rb-IgG (Raju et al. 2000). In our analysis of rRb-IgG we could not detect any NGNA sialic acid form, confirming again the observation that the glycosylation of rRb-IgG produced in HEK293 cells is closer to human IgG N-glycosylation.

The N-glycan structures described for nonrecombinant human IgG are mostly complex-type including core fucose. These N-glycan structures are the same described for rRb-IgGs expressed in HEK293, a human cell line, in contrast to the N-glycan structures of nonrecombinant Rb-IgGs. Those differences between human and Rb-IgG N-glycans were noted previously (Raju et al. 2000). Here we described the differences in the N-glycans of nonrecombinant and rRb-IgGs, and the similarities in those same glycan structures between human IgGs and rRb-IgGs produced in human cells. We concluded that the N-glycans added to the rRb-IgGs produced in human cells (HEK293) use the glycosylation machinery of the human cells and are not related to the primary sequence of the rIgGs. The hypothesis that IgG glycosylation depends on the host cell line has been previously suggested by Raju et al. (2000), and confirmed by Hossler et al. (2009). Nallet et al. (2012) showed that the human IgG produced in HEK293 cells had similar glycosylation profiles reported in the literature for nonrecombinant human IgGs.

O-Glycans from nonrecombinant Rb-IgGs were described before (Kabir and Gerwig 1997) as two trisaccharides, GalNAc(1)Gal(1) Neu5Gc(1) and GalNAc(1)Gal(1)Neu5Ac(1), at an 87:13 ratio. Their data also suggested that both trisaccharides were monosialylated as no signals due to disialylation were detected. In contrast, in our study, the O-glycans present in rRb-IgG produced in HEK293 cells were shown to be tetrasaccharide core 1 structures, and mostly disialylated, featuring only NANA as sialic acid type. In addition, we detected masses corresponding to the monosialylated or nonsialylated core 1 structures, though in lower abundance (Table I).

Fanger and Smyth (1972a) identified a glycan attached to the threonine residue next to the cysteine of the hinge region (SKPTCPPPGL) of nonrecombinant Rb-IgG by amino acid analysis and labeled it C2-glycopeptide. In our analysis of HEK293-derived rRb-IgG, we were able to corroborate the O-glycan binding site on the threonine with the sequence motif XPTCPPPX by two different methods (MS-glycopeptide analysis and enzymatic digestion), the same threonine residue described before for nonrecombinant Rb-IgGs.

Again, the natural O-glycosylation site is conserved upon recombinant expression and accordingly O-glycosylated, however, without NGNA sialic acids but rather with NANA sialic acids as present in human IgGs. This confirms the already defined hypothesis that N- as well as O-glycosylation depends on the host cell line.

For site-directed labeling of rRb-IgGs we applied the SrtA enzymatic technology as already described (Jacobitz et al. 2017; Antos et al. 2016): gram-positive bacteria use SrtA cysteine transpeptidase enzymes to covalently attach proteins to their cell wall and to assemble pili. *Staphylococcus aureus* SaSrtA enzyme became a valuable biochemical reagent because of its ability to sequentially cleave and

Table II. N-glycosylation site and glycan structures after HPLC–MS analysis of the tryptic digested N-glycan containing peptides including relative amounts. Monosaccharide symbols follow the SNFG (symbol nomenclature for Glycans) system (PMID 26543186, *Glycobiology* 25:1323–1324, 2015) details at NCBI. N-linked glycan nomenclature within the table is based on Reusch et al. (2015); however, bisecting GlcNAc was not present in the Reusch study, here bisecting GlcNAc is indicated by the acronym +N for the respective N-glycans

			Relative abundance [%]			
N-linked glycan structure	N-linked glycan nomenclature	Theoretical monoisotopic mass of the (glyco-) peptides (Da)	MAb<xxx>rRb-1G9-IgG	MAb<xxx>rRb-1A4-IgG	MAb<xxx>rRb-3G3-IgG	MAb<xxx>rRb-2F2-IgG
Peptide EQQFNSTIR (nonglycosylated)	-	1121.55	<0.1	<0.1	<0.1	0.8
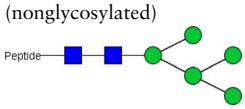	M5	2337.97	1.2	1.0	0.6	1.3
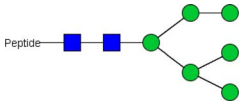	M6	2500.02	0.2	<0.1	0.2	<0.1
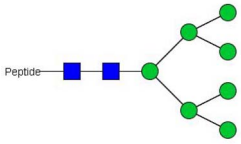	M7	2662.07	0.2	<0.1	0.2	0.2
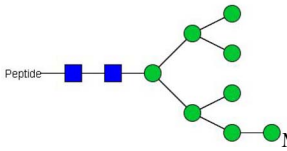	M8	2824.13	0.1	<0.1	0.2	<0.1
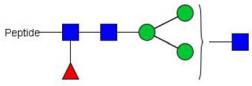	G0F-N	2363.00	3.8	3.8	3.5	4.5
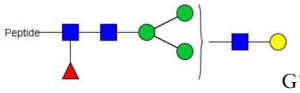	G1F-N	2525.05	0.5	0.7	0.6	0.6
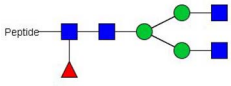	G0F	2566.08	63.0	59.2	57.2	66.1
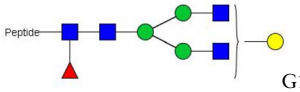	G1F	2728.13	24.6	28.0	28.3	20.9
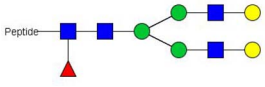	G2F	2890.19	3.3	3.9	5.3	2.5
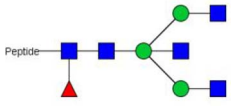	G0F + N	2769.16	1.1	1.0	0.9	0.9
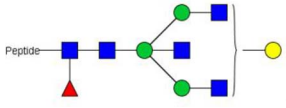	G1F + N	2931.21	0.6	0.7	0.6	0.5
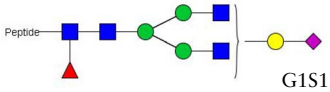	G1S1F	3019.23	0.7	0.6	1.2	0.6
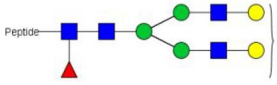	G2S1F	3181.28	0.4	0.3	0.8	0.1

ligate biomolecules together in vitro via covalent peptide bond. For generating biotinylated Fab fragments from rRb-IgG, an SaSrtA-Tag (LPETG) was included in the upper hinge region, in direct contact to the O-glycosylation site found for the rRb-IgGs. Previously, Tsay et al. (1980) described that nonrecombinant Rb-IgG molecules were found to be more resistant to the action of papain due to O-glycosylation.

Accordingly, we were not able to remove the O-glycans from rRb-IgGs completely by enzymatic methods, but we could remove the majority of sialic acids. In addition, we proved that the presence of sialic acid (charged saccharide) on O-glycan structures near the cleavage site decreases the cleavage efficacy of the SrtA enzyme, as the cleavage efficiency (measured as yield of purified biotinylated Fab-fragment) increased 5-fold after removing the sialic acids from the O-glycans. This suggests that charged sugar moieties could hinder protease activity, as their removal enhances that activity. Regarding the SrtA reaction products, more heavily O-glycosylated structures were prevalent in uncleaved Fc vs. cleaved Fc.

Replacement of the hinge threonine directly downstream of the SrtA site by alanine allowed an almost complete Fab fragment cleavage after 18 h incubation. This confirms the identity of the O-linked glycosylation site on Rb-IgG and shows that the O-glycan sialylated structure is sterically hindering SrtA (protease) access to the hinge region.

In conclusion, the current study analyzed the N- and O-glycans of various rRb-IgGs expressed in HEK293 cells. We were able to detect and quantify 13 different N-glycan and three different O-glycan structures and identify their positions. In our analysis of rRb-IgG we found that not only the N-glycosylation but also the O-glycosylation of rRb-IgG produced in HEK293 cells is closer to the human IgG glycosylation forms, confirming the already determined hypothesis that the host cell defines the glycosylation of the recombinant produced IgGs. Furthermore, we demonstrated that the O-glycosylation site present in rRb-IgG, which is about 50% glycosylated and sialylated, considerably affects the SrtA protease activity when located in close proximity to the cleavage site. Introduction of a point mutation at this position overcame this restriction, confirming the hypothesis that the O-glycan affects the SrtA activity, probably due to steric hindrance. Accordingly, mutation of the O-glycan site in order to avoid protease activity restrictions close to the IgG hinge region is recommended. We described here the detailed N- and O-glycan composition and glycosylation sites of rRb-IgGs and corroborated the hypothesis that the glycosylation of recombinant IgGs is completely dependent on the species of the expression system. This finding, and the determination of a steric hindrance for protease activity due to the presence of O-glycans close to the cleavage site, should be considered in any recombinant produced IgG for diagnostic or therapeutic purposes.

Materials and methods

Materials

Tris(hydroxymethyl)aminomethane hydrochloride, hydrochloric acid (HCl), guanidine hydrochloride, sodium hydroxide solution, 50% in H_2O (NaOH), sodium borohydride, powder, ≥98.0% ($NaBH_4$), iodomethane (MeI), dimethyl sulfoxide anhydrous, ≥99.9% (DMSO) and Neuraminidase Agarose (from *Clostridium perfringens*, Type VI-A) were obtained from Sigma–Aldrich (Taufkirchen, Germany). Iodoacetic acid (IAA), sodium salt and acetic acid (AcOH) glacial 100% were obtained from Merck (Darmstadt, Germany). Recombinant trypsin (proteomics grade), 1,4-dithiothreitol (DTT), ethylenediaminetetraacetic acid (EDTA), recombinant SrtA (amino acid sequence identical to UniProt Accession Nr. Q2FV99, with addition of C-terminal hexa-His-tag, expressed in *E. coli* and purified by immobilized metal affinity and size exclusion chromatography) and G4-EBES-K(Bi) peptide were obtained from Roche (Penzberg, Germany). RapidPNGase F from New England BioLabs (Frankfurt am Main, Germany). OpeRATOR™ and SialEXO™ were obtained from Genovis AB (Lund, Sweden). Trifluoroacetic acid (TFA) and formic acid (FA, 99%) were UPLC/MS grade and purchased from Biosolve Chimie (Dieuze, France). Acetonitrile (ACN; ultra-gradient HPLC grade), H_2O (HPLC gradient grade) and methanol (MeOH; Baker analyzed, ultra LC/MS) were purchased from Mallinckrodt Baker (Griesheim, Germany). GE Healthcare illustra™ NAP™ Columns (NAP-5) were obtained from GE Healthcare (Freiburg, Germany). Cation exchange AG 50 W-X8 resin 100–200 mesh hydrogen form and micro Bio-Spin chromatography columns were purchased from Bio-Rad (Munich, Germany). Hypersep C18 columns were obtained from Thermo Fisher Scientific (Waltham, MA, USA). For the identification and characterization of the O-glycans, two different rRb-IgG fragments: MAb<xxx>rRb-3B9-F(ab′)2 and MAb<xxx>rRb-4B14-F(ab′)2 were used. For the confirmation and relative quantification of the O-glycans, as well as for the identification and relative quantification of the N-glycans, the following rRb-IgGs were used: MAb<xxx>rRb-1G9-IgG, MAb<xxx>rRb-1A4-IgG, MAb<xxx>rRb-3G3-IgG and MAb<xxx>rRb-2F2-IgG. The monoclonal mouse antibody MAb<xxx>M-II-F(ab′)2 was used as negative control, whereas EPO and fetuin were used as positive controls. For the mapping of the O-glycosylation site MAb<xxx>rRb-8F3-IgG and MAb<xxx>rRb-4H3-IgG were used, while the mouse IgG Mab<xxx>M-2.20.46-IgG served as negative control.

For the SrtA reactions, the following IgGs were used: MAb<xxx>rRb-4H11-IgG (SrtA upper hinge) and MAb <xxx>rRb/M-4H11-IgG (SrtA lower hinge) and Mab<xxx>rRb-4H11(T > A)-IgG (SrtA upper hinge, threonine to alanine mutation).

Methods

Transient gene expression of the recombinant IgGs in HEK293-F cells

The coding sequences of heavy and light chains of MAb<xxx>rRb-4H11-IgG (SrtA upper hinge), MAb <xxx>rRb/M-4H11-IgG (SrtA lower hinge), rabbit and rabbit/mouse chimeric monoclonal antibodies featuring SrtA tags (LPETG) at different sites, were cloned separately into a standard mammalian expression vectors containing a CMV promoter. Both plasmids encoding heavy and light chain were cotransfected into suspension-adapted human embryonic kidney HEK293-F cells (Thermo Fischer Scientific). HEK293-F cells were cultured in shaker flasks at 37°C in FreeStyle 293 expression medium (Thermo Fisher Scientific) under serum-free medium conditions. The cells were transfected at ~2×10^6 vital cells/mL with the expression plasmids (0.5 mg/L of cell culture) complexed by PEIpro (Polyplus, Illkirch, France) transfection reagent (1.3 mL/L cell culture) in PBS buffer. The culture supernatant was collected at day 7 post-transfection by centrifugation. IgG was purified via one-step protein A affinity purification (HiTrap MabSelect SuRe, GE Healthcare) according to the supplier's instructions.

Reductive β-elimination of O-glycans

O-Glycans were released by reductive alkaline β-elimination by a modified version of the protocol described by Anumula and Taylor

(1992). One hundred micrograms of IgG were buffer-exchanged using Nanosep® Centrifugal Devices with Omega™ Membrane 10 K cutoff membrane. Samples were washed two times with 500 µL ultrapure H2O and finally concentrated >10 µL. Next, filled up to 100 µL incubated with 50 mM sodium hydroxide and 1 M sodium borohydride and incubated for 16–18 h at 50°C in a screw-cap vial. The reaction was quenched by several additions of 1 µL of 50% glacial acetic acid. The addition of 50% glacial acetic acid was repeated until bubbles were no longer formed after addition.

Cation exchange purification of the O-glycans

In order to separate the glycans from the positive-charged cations resulting from the used reagents, amino acids, peptides and other contaminants, the samples were purified using a cation exchange AG 50W-X8 resin 100–200 mesh. For this purpose, the micro Bio-Spin chromatography columns were packed up with a slurry of the resin, which was prepared by the addition of H_2O. The columns were then transferred in vials, centrifuged until the H_2O was eluted and transferred into new vials. Then the samples were loaded, centrifuged for 1 min to elute, and the eluents were finally dried in a SpeedVac until a white precipitate appeared at the bottom of each vial. The released glycans were further purified from borate by SpeedVac drying after repetitive addition (3–4 times) of 50 µL 1% AcOH in MeOH.

Permethylation of the released O-glycans

The dried released O-glycans were solubilized by the addition of 20 µL of anhydrous dimethyl sulfoxide (DMSO). Then another 20 µL of DMSO was added, followed by the addition of 20 µL sodium hydroxide (NaOH) in anhydrous DMSO (prepared separately). Ten microliter iodomethane (MeI) were added to each sample, and the reaction mixture was incubated for 5–10 min. The last three steps (addition of NaOH in anhydrous DMSO, MeI addition and incubation) were repeated once more. The reaction was quenched by the addition of 1 mL 0.1% AcOH. The samples were finally purified on the Hypersep C18 columns by eluting twice with 200 µL of 75% ACN in H_2O and by applying vacuum, and finally they were concentrated in a SpeedVac.

Analysis of released O-glycans by MS

For the mass spectrometric analysis of the released O-glycans, 20 µL of the permethylated glycan solution were transferred with a multichannel pipette to a 96-well plate (Abgene, Blenheim, UK) and 5 µL of 20% ACN solution containing 1% FA were added and mixed thoroughly (directly prior to the measurement). All measurements were performed in positive-ion mode with an Orbitrap Velos instrument from Thermo Scientific (Bremen, Germany) equipped with a TriVersa NanoMate robot from Advion (Harlow, UK). Resolution of the MS was set to 30,000 and the acquisition time per sample to 2 min. The NanoMate robot settings were as follows: 1.5 kV electrospray voltage, gas pressure 0.5 psi, contact closure 1 s.

Tryptic peptide mapping

For the detection and quantification of glycosylation within the molecule, the IgGs were digested with trypsin. First, they were denatured in 0.4 M Tris-HCl, 8 M Gua-HCl, at pH 8.5 by diluting 280 µg of IgG in a total volume of 300 µL. For reduction, 10 µL of 0.1 g/mL DTT were added and incubated at 50°C for 1 h. After alkylation of free cysteines by adding 0.33 g/mL IAA and incubation at room temperature in the dark for 30 min, the buffer was exchanged to digestion buffer (0.1 M Tris-HCl, pH 7.0) by application onto a NAP-5 filtration column. Subsequently, the NAP-5-eluate (500 µL) was mixed with 10 µL of a solution of 0.25 mg/mL trypsin in 10 mM HCl and incubated at 37°C for 18 ± 2 h. The digest was stopped by adding 50 µL of a 10% TFA solution.

Analysis of proteolytic peptides by liquid-chromatography MS

The tryptic peptide mixture was separated by RP-UPLC (ACQUITY, Waters, Manchester, UK) on a C18 column (BEH C18 1,7 µm 2,1 × 150mm; Waters, Manchester, UK) and the eluate was online analyzed with a LTQ Orbitrap Velos electrospray mass spectrometer (Thermo Scientific). The mobile phases consisted of 0.1% FA in H_2O (solvent A) and 0.1% FA in ACN (solvent B). The chromatography was carried out using a gradient from 1% to 35% solvent B in 45 min and finally from 35% to 80% solvent B in 3 min using a flow rate of 300 µL/min. UV absorption was measured at a wavelength of 220 nm. About 3.5 µg digested protein were applied. UPLC-system and mass spectrometer were connected by PEEK-capillary tubes. Data acquisition was controlled by Xcalibur software (Thermo Scientific, V2.1.0.1140). Parameters for MS detection were adjusted according to general experience available from peptide analysis of rIgGs.

Data analysis for the identification and quantification of N- and O-linked glycans

Theoretical glycopeptide masses in Da were calculated by adding a list of possible O-glycan or N-glycan structures to the theoretical tryptic peptide mass. Glycopeptides of interest were than manually identified by comparing experimental mass vs. theoretical mass. In the supplementary data (Supplementary Tables SI and SII), detected glycopeptides are listed, including mass deviation to theoretical mass in parts per million. For the quantification, specific ion current (SIC) chromatograms of identified glycopeptides were generated on the basis of their monoisotopic masses and detected charge states using the software BYOLOGIC® (Version 3.3-316 x64, Protein Metrics, Cupertino, USA). The relative amounts of the different detected glycopeptides were calculated from the manual integration results of the different glycopeptide peaks.

O-glycosylation site mapping using an O-glycan dependent endoprotease

For comparison of the results of the O-glycosylation site determination, the IgGs were digested using an O-glycan-specific protease (OpeRATOR™, Genovis) that cleaves at the N-terminus of O-glycosylated serines or threonines with removal of the sialic acids, according to manufacturer's protocol. In short, the IgGs were dissolved in digestion buffer (20 mM Tris, pH 6.8) to a concentration of 2 mg/mL. One unit of sialidase (SialEXO™, Genovis) was added per 1 µg IgG. Then 1 unit OpeRATOR™ was added per 1 µg IgG and the samples were incubated at 37°C overnight. The samples were further analyzed with intact HPLC–MS analysis.

Desialylation of hinge O-glycans and SrtA reaction

Neuraminidase Agarose beads were washed five times (by centrifugation) with twice the volumes each of H_2O and 0.1 M sodium acetate pH 5.0. Buffers of IgG solutions were exchanged via dialysis (5 h, 10 kDa MWCO) to 0.1 M sodium acetate pH 5.0 and IgG

concentrations adjusted to 3.3 mg/mL. Approximately 2.5 U of Neuraminidase Agarose beads were added to 5 mg IgG-solution and incubated at 37°C overnight. Desialylated IgG were recovered by filtration (0.22 µm centrifugal filter) and analyzed by absorbance at 280 nm, size exclusion chromatography (GE Superdex 200 increase) and ESI–MS.

SrtA reactions on SrtA upper hinge and lower hinge constructs were performed as follows: buffers of IgG solutions were exchanged via dialysis (3 h, 10 kDa MWCO) to 50 mM Tris, 150 mM KCl pH 8.0. Dialysates were concentrated via Amicon Ultra (10 kDa MWCO), absorbance at 280 nm determined, and final concentrations adjusted to 9 mg/mL in a 50 mM Tris, 150 mM KCl pH 8.0 solution containing 5 mM $CaCl_2$, 3 mM G4-EBES-K(Bi) Peptide and 1.44 U SrtA per mg IgG. Reaction mixes were incubated at 37°C under agitation for the times indicated and SrtA reactions were stopped by addition of EDTA ad 5 mM. The formation of Fab and F(ab′)2 fragments was analyzed via size exclusion chromatography. Each stopped SrtA reaction mix was added to a suspension of complete His-Tag Purification Resin (Roche), equilibrated with 4 × 8 volumes of 50/150/5 mM Tris/KCl/EDTA pH 8.0. The slurry was incubated under agitation (rolling) at RT for 1 h.

Method for intact HPLC–MS analysis

For the intact mass spectrometric analysis of O-glycosylated IgGs (including samples treated with Operator™ as described above), the samples were diluted in 20/50/5 mM Tris/NaCl/EDTA pH 7.5 to a sample concentration of 200 µg/mL. For 10 µg of sample, 1 µL of RapidPNGase F (NewEnglandBiolabs) was added. After 1 h incubation at 50°C the samples were diluted to 50 µg/mL in H2O. For analyzing reduced samples, TCEP was added to a final concentration of 5 mM and incubated for 20 min at 37°C.

The N-deglycosylated mixture was separated by using a Waters Acquity UPLC with a Waters Acquity UPLC Protein BEH C4 (2.1 mm × 100 mm; 300 Å; 1.5 µm) with a gradient from 0.1% FA in H_2O to 0.1% FA in ACN at a flowrate of 200 µL/min. The eluting proteins were ionized with a Zspray (ESI source) and then measured on a Waters Xevo G2-S ToF. The spectra were acquired in positive resolution mode and the mass range was set to 450–4500 m/z. MaxEnt1 was used to deconvolute the combined raw spectra.

Supplementary data

Supplementary data for this article is available online at http://glycob.oxfordjournals.org/.

Acknowledgments

We would like to thank the group of Tobias Oelschlaegel for their help and fruitful discussions on Sortase cleavage of rabbit and chimeric antibodies. We thank also Michael Gerg's group for the production of all different recombinant rabbit IgGs used in this report and Anne-Laure Simon for establishing the methods for cleavage and purification of rRb-IgG in our lab.

References

Antos JM, Truttmann MC, Ploegh HL. 2016. Recent advances in sortase-catalyzed ligation methodology. *Curr Opin Struct Biol*. 38:111–118.

Anumula KR, Taylor PB. 1992. A comprehensive procedure for preparation of partially methylated alditol acetates from glycoprotein carbohydrates. *Anal Biochem*. 203:101–108.

Beerli RR, Grawunder U. 2017. Enzyme-based strategies to generate site-specifically conjugated antibody drug conjugates. In: Grawunder U, Barth S, editors. *Next Generation Antibody Drug Conjugates (ADCs) and Immunotoxins. Milestones in Drug Therapy*. Cham (Switzerland): Springer. p. 85–106.

Dashivets T, Thomann M, Rueger P, Knaupp A, Buchner J, Schlothauer T. 2015. Multi-angle effector function analysis of human monclonal IgG glycovariants. *PLoS One*. 10:e0143520.

de Haan N, Falck D, Wuhrer M. 2020. Monitoring of immunoglobulin N- and O-glycosylation in health and disease. *Glycobiology*. 30:226–240.

Fanger MW, Smyth DG. 1972a. The oligosaccharide units of rabbit immunoglobulin G. Multiple carbohydrate attachment sites. *Biochem J*. 127:757–765.

Fanger MW, Smyth DG. 1972b. The oligosaccharide units of rabbit immunoglobulin G. Asymmetric attachment of C2-oligosaccharide. *Biochem J*. 127:767–774.

Hossler P, Khattak S, Li ZJ. 2009. Optimal and consistent glycosylation in mammalian cell culture. *Glycobiology*. 19:936–949.

Jacobitz AW, Kattke MD, Wereszczynski J, Clubb RT. 2017. Sortase transpeptidases: Structural biology and catalytic mechanism. *Adv Protein Chem Struct Biol*. 109:223–264.

Kabir S, Gerwig GJ. 1997. The structural analysis of the O-glycans of the jacalin-bound rabbit immunoglobulin G. *Biochem Mol Biol Int*. 42:769–778.

Köhler G, Hengartner H, Shulman MJ. 1978. Immunoglobulin production by lymphocyte hybridomas. *Eur J Immunol*. 8:82–88.

Lloyd KA, Steen J, Amara K, Titcombe PJ, Israelsson L, Lundström SL, Zhou D, Zubarev RA, Reed E, Piccoli L *et al*. 2018. Variable domain N-linked glycosylation and negative surface charge are key features of monoclonal ACPA: Implications for B-cell selection. *Eur J Immunol*. 48: 1030–1045.

Mizuochi T, Taniguchi T, Shimizu A, Kobata A. 1982. Structural and numerical variations of the carbohydrate moiety of immunoglobulin G. *J Immunol*. 129:2016–2020.

Nallet S, Fornelli L, Schmitt S, Parra J, Baldi L, Tsybin YO, Wurm FM. 2012. Glycan variability on a recombinant IgG antibody transiently produced in HEK-293E cells. *N Biotechnol*. 29:471–476.

Patel TP, Parekh RB, Moellering BJ, Prior CP. 1992. Different culture methods lead to differences in glycosylation of a murine IgG monoclonal antibody. *Biochem J*. 1:839–845.

Popp MW, Antos JM, Grotenbreg GM, Spooner E, Ploegh HL. 2007. Sortagging: A versatile method for protein labeling. *Nat Chem Biol*. 3: 707–708.

Raju TS, Briggs JB, Borge SM, Jones AJS. 2000. Species-specific variation in glycosylation of IgG: Evidence for the species-specific sialylation and branch-specific galactosylation and importance for engineering recombinant glycoprotein therapeutics. *Glycobiology*. 10:477–486.

Reusch D, Haberger M, Maier B, Maier M, Kloseck R, Zimmermann B, Hook M, Szabo Z, Tep S, Wegstein J *et al*. 2015. Comparison of methods for the analysis of therapeutic immunoglobulin G Fc-glycosylation profiles–part 1: Separation-based methods. *MAbs*. 7:167–179.

Sutton BJ, Phillips DC. 1983. The three-dimensional structure of the carbohydrate within the Fc fragment of immunoglobulin G. *Biochem Soc Trans*. 11:130–132.

Taniguchi T, Mizuochi T, Beale M, Dwek RA, Rademacher TW, Kobata A. 1985. Structures of the sugar chains of rabbit immunoglobulin G: Occurrence of asparagine-linked sugar chains in Fab fragment. *Biochemistry*. 24:5551–5557.

Tsay DD, Shaw AR, Schlamowitz M, Mandy WJ. 1980. Binding, fractionation, and papain susceptibility of groups d and e rabbit IgG allotypes. *J Immunol*. 124:2669–2674.

Yamaguchi Y, Barb AW. 2020. A synopsis of recent developments defining how N-glycosylation impacts immunoglobulin G structure and function. *Glycobiology*. 30:214–225.